

An Investigation into a Geocell- Reinforced Slope in The Unsaturated Numerical Model

Behnam Mehdipour^a, Hamid Hashemalhosseini^{*,b}, Bahram Nadi^c, Masoud Mirmohammad sadeghi^d

^{a,c} *Department of Civil Engineering, Najafabad Branch, Islamic Azad University, Najafabad, Iran.*

^b *Faculty of Civil Engineering, Isfahan University of Technology, Isfahan, Iran.*

^d *Faculty of Civil Engineering, Isfahan Higher Education and Research Institute, Isfahan, Iran.*

Received 23 July 2018, Accepted 29 November 2018

Abstract

Considering the unsaturation conditions of soil significantly helps to produce relatively real results. Numerical methods have been assumed as conventional methods in soil mechanics to examine soil behavior. However, the accuracy of numerical methods dramatically depends on applying the appropriate behavioral model to solve problems. One of the known elastoplastic models for unsaturated soils is the Barcelona Basic Model which is added to FLAC2D software through codification. Geocell-reinforced slope functions as a beam in the soil due to the three-dimensional nature of the reinforcement, i.e. height are included. Furthermore, the reinforcement causes a reduction in slope displacement and an increase in the factor of safety of slope due to its bending characteristics including the moment of inertia and consequently bending strength. Moreover, soil unsaturated conditions are applied to the modeling and suction variations in the soil are incorporated. This makes the maximum horizontal displacement of slope occur in the upper part of the Geocell layer while the horizontal displacement values for the slope height are substantially reduced below the Geocell layer. Increasing suction, geocell axial force declines by at most 18.5%. As overhead pressure increases, there is an increase in the force concentrated at the soil-geocell interface and the tensile force is consequently enlarged in reinforcements.


Keywords: *Unsaturated Soil, Barcelona Basic Model, Suction, Geocell, FLAC2D*

1. Introduction

Construction projects by more advanced technologies are increasingly developing. One of the restrictions on such projects is the inappropriateness of the project implementation site as the structure foundation. Recognition of the land appropriateness to construct the foundation requires the knowledge and expertise of engineers and researchers about the soil behavior in different conditions and states. In other words, researchers should be aware of the variation in soil behavior under different circumstances so as to provide a qualitative and quantitative evaluation of the soil behavior in different conditions. However, the principles of classic soil mechanics founded by

Carl Tarzaghi are mostly associated with saturated soils [1]. Unsaturated soil is not a specific type of soil but rather it is a state of soil that can occur for all types of soil based on the filling fluid. Saturation or unsaturation in any region is affected by environmental factors, namely rainfall, evaporation, and rise of groundwater level. In other words, all soils are subjected to either wetting or drying. Therefore, change in the state of pore-water pressure and the occurrence of unsaturated conditions are probable for all soils [2].

Full drying conditions of soil, particularly for granular soil, might experience a reduction in the factor of safety by wetting and moisture absorption at the end of construction stages. Moreover, since

 *Corresponding Author: Email: Address: hashemalhosseini@cc.iut.ac.ir

the shear strength of the soil is drastically affected by the degree of soil saturation, it is important to consider correct conditions of saturation or unsaturation of soil once investigating the soil behavior. In fact, although the design is more simplified in geotechnical engineering by not considering unsaturated soil conditions, it increases most of the construction costs [3].

In recent years, tremendous advancements have been made in the field of unsaturated soil whereby valid results and models have been developed. However, in some of the proposed models, there are defects and ambiguous points including disagreement between experimental and empirical results and also lack of harmony between the proposed models for saturated and unsaturated states of soil, requiring further investigation and study [1].

Fredlund and Morgenstern in 1978 [4] proposed a relation to express the shear strength of unsaturated soils where it properly separated the shear strength due to effective stress from the shear strength induced by net stress. In recent years, the effective stress method has been of great interest to many researchers to determine the shear strength of unsaturated soils [5-9].

In 1998, a relation was proposed based on effective stress, cohesion, and internal friction angle of soil to express the shear strength of unsaturated clay [9]. On the other hand, the effective stress of unsaturated soils is in direct proportion to the extent of matric suction within the soil.

In this regard, Alonso et al. were among pioneers and their study attracted a great deal of attention such that one can find a large number of basic models in the respective scientific references.

This model, as the most known model proposed in the analysis of unsaturated soil, functions on the basis of three major concepts including state surfaces, soil critical state, and empirical tests. This model can be referred to as to the development of the critical state in the unsaturated state considering the effect of the suction phenomenon [10].

The result of most studies are summarized in the following three parts:

A- Fundamentals of stress states and principal variables employed to create numerous models

B- Precise analysis of basic models and investigation of their strengths and weaknesses
C- Progress in the modeling unsaturated soil [1].

Different studies have been conducted on reinforced soil slope. The effect of length and distance of reinforcements on the behavior of reinforced soil slope has been widely examined. The obtained results revealed that as the distances between reinforcements increase, the available load in reinforcement layers and consequently wall deformation increase as well. To investigate the failure mechanism of geosynthetic-reinforced soil slope and evaluate the design hypothesis and design methods for such walls, numerical and experimental studies have been carried out showing that the failure surface is different from the propagation of failure region but rather its location is dependent on geometry, strength, and stiffness of reinforcement elements [11-16]. Employing geocell to reinforce soils has broad applications as an effective and rapid method in civil projects. Geocell-reinforced soil is chiefly used to resist static and cyclic loads. In fact, this reinforcement is used to increase the load-bearing capacity of soft soil and decrease settlement and displacements of slopes. Geocell functions as a layer of confining soil and prevent the soil from moving outward to the loading region. Furthermore, soil swelling is reduced which leads to some variations in the factor of safety of slope. Geocell increases the bending, tensile, and shear strength of the soil and, due to its height, functions as a beam providing a moment of inertia and consequently bending strength. Although bending stiffness is low with respect to thickness, it can diminish the deformations of layers and cause a reduction in the settlement of the soil-structure system [17,18]. Fakher and Jones investigated the effect of bending stiffness of geogrid reinforcement using Flac software. Their results show that although bending stiffness is low with respect to the small thickness of the geogrid layer, it can diminish the deformation of the geogrid layer and consequently decrease the system settlement [19].

Zhang et al. [20, 21] simulated the performance of geocell reinforcement considering the resistance of contact surface between soil and geocell and assumed the geocell reinforcement as a beam on an elastic bed.

Dash et al. [22] observed through an experimental effort that the geocell layer functioned as a beam with bending behavior. Their results illustrated that as the height of the geocell layer increases, the behavior of deep beam becomes dominant in the geocell layer. Yang et al. [23] indicated that geocell benefits form a relatively high bending strength where it is necessary to incorporate bending stiffness in modeling the geocell layer. The present study uses a beam element in Flac2D software to incorporate the properties of the geocell layer in the simulation of geocell reinforcement.

2. Theory

2.1. Barcelona basic model

The present study has used the Barcelona basic model that works elastoplastically and is applied to express the stress-strain of unsaturated soils based on stiffening plasticity. This model was first proposed by Alonso in 1990 at Polytechnic University of Catalonia. It is founded on the basis of the Cam-clay model and capable of expressing many principle facets of the behavior of unsaturated soils, namely silty soils, clayey sands, sandy clay, and clay with low plasticity. It is worth noting that this model has been proposed with the purpose of expressing the behavior of partially saturated soil with low or medium inflation capability. This model is one of the most known proposed models to analyze unsaturated soils which is based on three major principles including state surfaces, soil critical state, and empirical tests. This model can be referred to as to the development of the critical state in the unsaturated state considering the effect of the suction phenomenon. The Barcelona basic model has two independent stress variables in the form of net stress and soil suction.[10]

$$\sigma_{ij}^- = \sigma_{ij} - \partial_{ij} u_{ij} \quad (1)$$

$$S = u_a - u_w \quad (2)$$

Where σ_{ij}^- stands for net stress tensor, σ_{ij} denotes total stress tensor, ∂_{ij} is Kronecker delta, S is soil suction, u_a stands for pore-air pressure, u_w is pore-water pressure. The relations of Barcelona basic model are written based on four variables

including net mean stress P, deviatoric stress q, nest suction S, and specific volume v.

$$P = \frac{\sigma_1 + \sigma_2 + \sigma_3}{3} \quad (3)$$

$$q = \frac{1}{\sqrt{2}} \sqrt{(\sigma_1 - \sigma_2)^2 + (\sigma_2 - \sigma_3)^2 + (\sigma_1 - \sigma_3)^2} \quad (4)$$

Where $\sigma_1, \sigma_2, \sigma_3$ are the principal stresses of soil. If the soil is isotopically loaded at constant suction until the net mean stress across the normal consolidation line (NCL), the specific volume is obtained by the following relation.

$$v = N(s) - \lambda(s) L n \frac{P}{P^c} \quad (5)$$

Here $\lambda(s)$ is the stiffness parameter along the normal consolidation line at constant suction S, and P^c stands for the reference pressure in $v = N(s)$. If unloading and reloading occur at constant suction, then the soil behavior is assumed as elastic. Constant suction is considered for all surfaces in the Barcelona basic model. The stiffness parameter on the normal consolidation line is defined at a constant suction as follows:

$$\lambda(s) = \lambda(0) [(1-r) \exp(\beta s) + r] \quad (6)$$

r is a parameter defining the maximum soil stiffness and β controls the soil stiffness increase rate induced by suction. Similar to the actions due to the applied net stress, suction also yields elastic and plastic strains. Once the soil reaches the already-experienced maximum suction, the irrecoverable strain is initiated [10]. In the Barcelona basic model, partial volumetric strain $d\varepsilon_v$ depends on the variations of a net mean stress, given as the following relation.

$$d\varepsilon_v = d\varepsilon_1 + d\varepsilon_2 + d\varepsilon_3 \quad (7)$$

$$d\varepsilon_q = \frac{\sqrt{2}}{3} \sqrt{(d\varepsilon_1 - d\varepsilon_2)^2 + (d\varepsilon_2 - d\varepsilon_3)^2 + (d\varepsilon_1 - d\varepsilon_3)^2} \quad (8)$$

The partial strain induced by net mean and deviatoric stresses are divided into two components, namely elastic strain $d\varepsilon^e$ and plastic strain $d\varepsilon^p$. On the other hand, the partial volumetric strain, due to the suction decrease by wetting or the suction increase by drying, is found purely elastic.

$$d\varepsilon = (d\varepsilon^e + d\varepsilon^p)_p + (d\varepsilon^e + d\varepsilon^p)_s \quad (9)$$

This model consists of a suction decrease yield curve showing that the effect of the suction change on the soil state to reach the yield point is as important as the effect of variation in the net mean stress. The volumetric elastic strain is generated by the net mean stress in the elastic region.

$$d\varepsilon_{vp}^p = \frac{k}{v} \frac{dp}{p} \quad (10)$$

When the net mean stress meets the pre-consolidation stress P_0 at the constant suction S , the soil is still in the normal consolidation state and the total volumetric strain is obtained by eq(11).

$$d\varepsilon_{vp}^p = \frac{\lambda(s)}{v} \frac{dp_0}{P_0} \quad (11)$$

Therefore, the plastic volumetric strain is defined by the subtraction of the elastic volumetric strain from the total volumetric strain.

$$d\varepsilon_{vp}^p = \frac{\lambda(0) - k}{v} \frac{dp^*}{p^*} \quad (12)$$

Similarly, elastic, plastic, and total volumetric strains dependent on suction variations are given by relations (13), (14), and (15), respectively.

$$d\varepsilon_{vk}^p = \frac{k_s}{v} \frac{ds}{s + P_{atm}} \quad (13)$$

$$d\varepsilon_{vs} = \frac{\lambda(s)}{v} \frac{ds_0}{s_0 + P_{atm}} \quad (14)$$

$$d\varepsilon_{vs}^p = \frac{\lambda(s) - k_s}{v} \frac{ds_0}{s_0 + P_{atm}} \quad (15)$$

Thus, once the yield state occurs, the increment of pre-consolidation pressure and yield suction can be presented using stiffening rules, given by the following relations.

$$\frac{dp_0^*}{p_0^*} = \frac{v}{\lambda(0) - k} d\varepsilon_{vp}^p \quad (16)$$

$$\frac{ds_0}{s_0 + P_{atm}} = \frac{v}{\lambda(s) - k_s} d\varepsilon_{vp}^p \quad (17)$$

Here k_s is the stiffness parameter for suction change in the elastic region. In the states of total stress, deviatoric stress q defines the effect of shear stress. The Barcelona basic model suggests that the shear strength increases by suction. It is a general attribute of partially saturated soils which is obtained by adding apparent cohesion P_s .

$$p_s = k_s \cdot s \quad (18)$$

Here k defines the cohesion increase by suction increase. The critical state line at each constant suction (s) is horizontal in saturation conditions (Fig. 1). The respective equation for the critical state line is as follows:

$$f = q^2 - M^2(p + p_s)(p_0 - p) \quad (19)$$

where, M is the slope of the critical state line. The non-associated flow rule is applied to accurately estimate the correct value of k_0 .

$$\frac{d\varepsilon_s^p}{d\varepsilon_{vp}^p} = \frac{2q\alpha}{M^2(2p + p_s - p_0)} \quad (20)$$

Here α is the parameter of the non-associated flow rule. The strain caused by changing deviatoric stress is obtained by relation (21).

$$d\varepsilon_q^p = \frac{1}{3G} dq \quad (21)$$

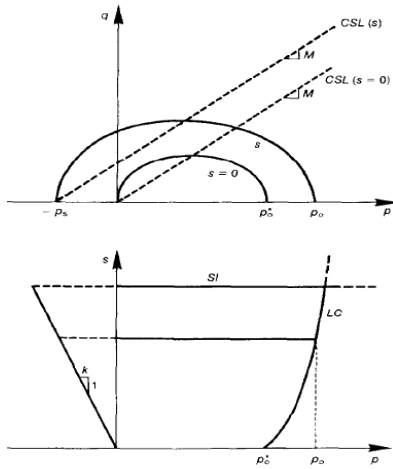


Figure 1. Failure surface in space (s, p, q) [10]

FISH is employed to codify the Barcelona basic model in FALC2D. The codification method of Barcelona basic model is very identical to the modified Cam-clay model.

2.2. Water-soil characteristic curve

Numerous functions have been proposed so far to describe a water-soil characteristic curve. The present study has benefited from the model proposed by Van Genuchten. This model is defined by relation (22).

$$\frac{\theta - \theta_r}{\theta_s - \theta_r} = \frac{1}{[1 + (\alpha\psi)^n]^m} \quad (22)$$

Here α , m , and n are fitting parameters. ψ stands for soil suction and θ_s, θ_r are residual water content and saturated water content, respectively. The slope of the curve is affected by m higher values of suction. m and n are correlated according to relation (23).

$$m = 1 - \frac{1}{n} \quad (23)$$

Replacing relation (23) in relation (22), the general relation for the function of the water-soil characteristic curve is obtained. Regarding this

relation, a certain amount of suction is reached for any specific degree of soil saturation [24, 25].

$$\frac{\theta - \theta_r}{\theta_s - \theta_r} = \frac{1}{[1 + (\alpha\psi)^n]^{-\frac{1}{n}}} \quad (24)$$

Values for relation (24) are represented in Table 1. They are based on SWCC curve with the regression $R^2 = 0.942$ (Fig. 2). By inserting the values of table 1 in relation 24, figure 2 is obtained.

Table 1. Parameters of the relation for water-soil curve [25]

θ_s	θ_r	$\alpha \text{ (m}^{-1}\text{)}$
0.48	0.1	0.3

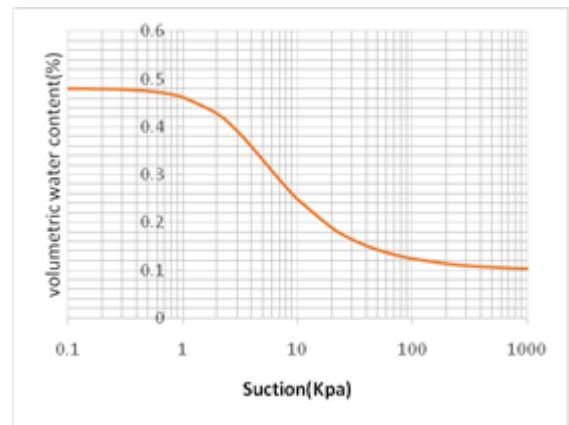


Figure 2. Water-soil characteristic curve

2.3. Geocell

Geocell reinforcement has tensile and shear force in the interface of soil and geocell. Furthermore, due to having a thickness and elasticity modulus, it offers a moment of inertia and consequently bending moment. As it can be observed in (Fig.2). T, M, and Q are tensile force, bending moment, and shear force of geocell, respectively. $q(y)$ is applied to the upper part of the geocell layer while $p(y)$ induced by the bed reaction is acted in the lower part of the geocell layer. h is the thickness of geocell reinforcement and $T(x)$ is the strength of the soil- geocell interface (Fig. 3).

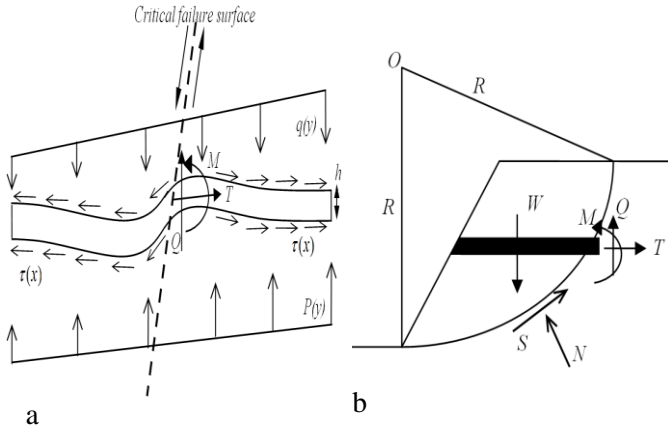


Figure 3. (a) Failure mechanism of geocell reinforcement, (b) acting forces on geocell reinforced slope.

Normal and shear forces causing the response of adjoining elements are calculated using the following equations at $t+\Delta t$ [26].

$$F_n^{(t+\Delta t)} = K_n u_n A + \sigma_n A \quad (25)$$

$$F_{si}^{(t+\Delta t)} = F_{si}^{(t)} + K_s \Delta u_{si}^{(t+0.5\Delta t)} A + \sigma_{si} A \quad (26)$$

where $F_n^{(t+\Delta t)}$ is the normal force at $t+\Delta t$, $F_{si}^{(t+\Delta t)}$ is the shear force at $t+\Delta t$, u_n stands for the absolute penetration of the adjoining element node perpendicular to the targeted surface, $\Delta u_{si}^{(t+0.5\Delta t)}$ is relative shear displacement, σ_n is normal stress, K_n and K_s are normal and shear stiffness, respectively, A is the specified area allocated to each node and σ_{si} is the extra shear stress due to the stress generated in the adjoining element. The values of normal and shear stiffness are calculated using the following relation [27,28].

$$k_n = k_s = 10 \times \max \left[\frac{k + \frac{4}{3} G}{\Delta z_{\min}} \right] \quad (27)$$

Here k is bulk modulus and G is soil shear modulus. Δz_{\min} is the width of the smallest adjoining zone in the normal direction.

3. Numerical Model

The Barcelona basic model is a soil behavioral model to investigate the reinforced slope. This model is added to the finite difference Flac software through codification. In FISH code written based on the triaxial test for validation of the Barcelona basic model, the generation algorithms of P, q, v, ϵ, S (suction) have been predicted. Soil properties are given in Table 2.

The conditions of numerical modeling are summarized in four main steps, namely generation of model geometry and reinforced slope, setting boundary conditions and respective stresses, running the program to approach initial equilibrium, and finally investigation of the factor of safety and deformation of reinforced slope and bending variations of geocell in the unsaturated state of soil. The concerned slope has a width of 50m and a height of 30m. The sensitivity analysis and several modeling have been conducted to select the optimum limit such that any further increase in the limit yields no change in results and merely increases the computational time. Due to the symmetry, only half of the slope has been modeled. The symmetry line is positioned on the right side of the model. To more precisely analyze the model as to determining the factor of safety (FOS) and deformation of the reinforced soil slope, a finer mesh is applied. Moreover, the mesh size becomes larger once moving away from the slope so as to reduce the computational time. The lower boundary of the model has been fixed against any movement and displacement in all directions while the vertical boundary is solely constrained in the horizontal direction (Fig.4). The investigated parameters to address the effect of geocell reinforcement on the factor of safety and failure surface are as follows: (u) depth of the first geocell layer measured from the slope top level, (N) number of geocell layers, (h) height of geocell layer, and (L) length of geocell layer. To simplify the obtained results, the dimensionless form of all available parameters have been expressed with respect to the slope height (e.g. u/H or L/H).

To study the effect of geocell-reinforced layer, the improvement factor (IF) is used, as given:

$$IF = \left[\frac{FOS_{reinforced}}{FOS_{unreinforced-drain}} \right] \quad (28)$$

Table 2. Model parameters [10]

Parameter	Value	Description
G	3.3MPa	Shear modulus
M	0.82	The slope of the critical state line
λ	0.14	The slope of the modified isotropic line
K	0.015	The slope of the elastic inflation line
β	16.4MPa ⁻¹	The parameter that controls the soil stiffness increase using suction.
r	0.26	The constant value associated with the maximum soil stiffness
k	1.24	Cohesion increase by suction increase
k_s	0.01	Elastic stiffness parameter for suction change
v	1.915	Poisson's ratio
p^c	0.043MPa	Reference pressure

The secant modulus of geocell (M) has been set 150 (kN/M) at a strain of 2.5%. Furthermore, the tensile strength and thickness of geocell have been considered 60 (kN/M) and 0.05m, and Modulus of elasticity is 20Mpa, In this study, the normal and the shear stiffness were calculated as 108 pa/m, respectively. The investigated non-reinforced clay slope has a factor of safety of 1.15 and a displacement of 15.6cm in dry soil. The foundation soil of slope is saturated but the soil of embankment is unsaturated. All of the models are used at the suction of 36kPa and moisture of 60%, according to SWCC.

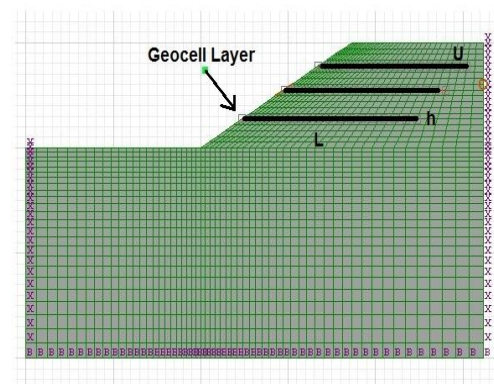


Figure 4. Schematic view of the slope with geocell

3.1. Validation

The Barcelona basic model has been applied to Flac software by making the following assumptions.

1. Net mean stress is equal to total mean stress, which is a practical assumption.
2. Soil suction is a variable affecting both soil strength and stiffness.

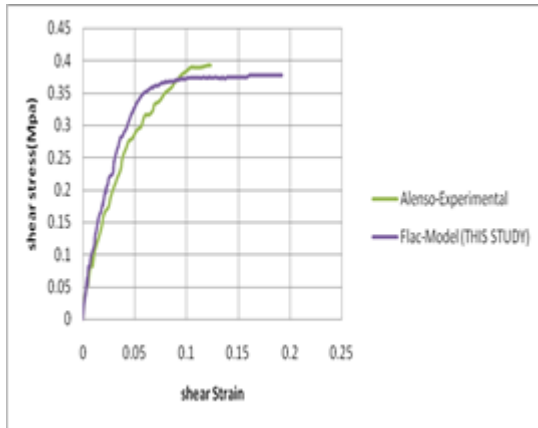


Figure 5. Validation of the generated model in Flac software using the Barcelona basic model (suction of 90kPa)

A single element with axisymmetric conditions is considered for the simulation to model triaxial tests on the soil of the reference model. Boundary conditions of the single element have been taken into account. In practice, the single element exhibits one quarter of the triaxial sample being tested, which has been fixed in two other directions. According to Fig. 5, the curve obtained in the study conducted by Alonso is negligibly different from the curve obtained from the results of Flac software where the error is less than 5%. The validation results suggest that the proposed model has an acceptable capability of explaining the behavior of unsaturated soil.

4. Effect of Number of Geocell Layers on the Stability of the Reinforced Slope

As shown in Fig. 6, an increase in the number of reinforcement layers enhances the factor of safety. Such a behavior can be attributed to the extension of the adjoining zone and higher frictional resistance at the soil- geocell interface. Therefore, higher horizontal shear stress occurs in the soil behind the failure surface. In these conditions,

bending stiffness and shear strength of reinforcements are also enhanced, thus avoiding horizontal displacements of soil. In U/H ratio (=0.6), the number of layers of IF factor increases by about 20% and there will be a significant decrease in a geocell layer with the increase of U/H ratio.

The improvement rate of the factor of safety based on the number of layers mainly depends on the depth of the first geocell reinforcement layer. This can be addressed as the ability of the first reinforcement layer to avoid the propagation of sliding surface which can consequently affect the overall slope stability. The performance of other geocell layers is largely associated with the improvement of the lateral deformation of slope (Fig. 7).

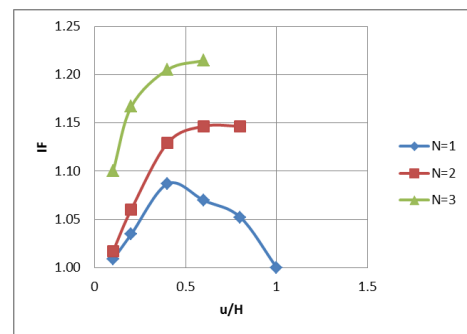


Figure 6. Variations in the improvement factor of slope against the number of geocell layers

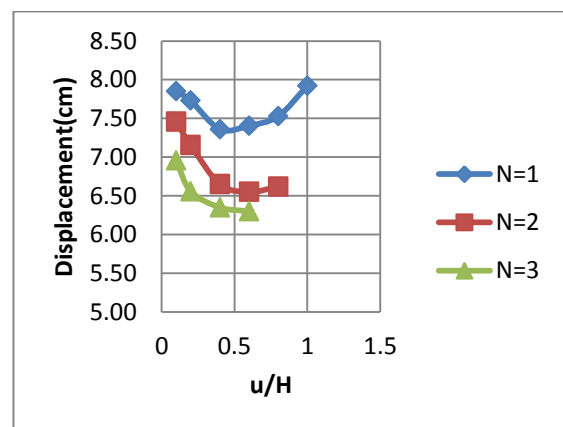


Figure 7. Displacement variations against the number of geocell layers

As can be observed in Fig. 7, an increase in u/H from 0.2 to 0.6 causes a reduction in slope

displacement by 22.6%. Therefore, the results reveal that the first geocell layer functions as a wide slap and yields the redistribution of load on a broader surface and reduction in the stress intensity. The first geocell layer dramatically transfers the force to the lower parts and consequently leads to force transfer to other geocell layers along with the enhancement of the stability performance.

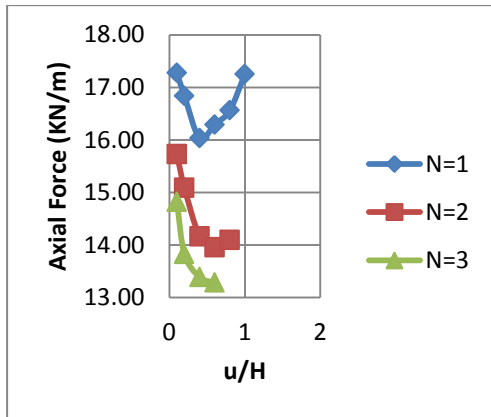


Figure 8. Variations in the axial force of the geocell layer versus the number of geocell layers

Based on Fig. 8, as the number of geocell layers increases, the axial force of the geocell layer is noticeably reduced. By increasing the geocell layers, the axial force between them is divided. The increase in soil overhead has increased the amount of mobilized force at the joint level of soil-geocell. As a result, the amount of tensile strength increases in the axial forces.

On the other hand, the first layer of the geocell can be used Considerably reduced the amount of horizontal displacement and shear strain in the height of the slopes.

In fact, receiving the main portion of forces in the first geocell layer, the moment of inertia is largely delivered to the first geocell layer and it is consequently diminished in other layers (Fig. 9).

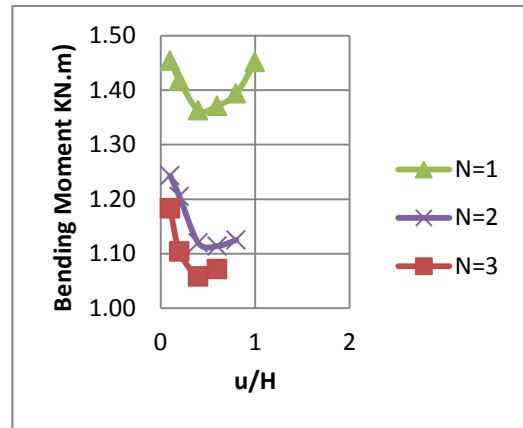


Figure 9. Variations of the bending moment in the geocell layer against the number of geocell layers

5. Effect of Length of Geocell Layers on the Stability of Reinforced Soil

Fig.10 shows the variations of the improvement factor of slope affected by the length of the reinforcement layer. The obtained results demonstrate that as the reinforcement layer increases in length, the factor of safety is enhanced as well. This is attributed to the increase in restraining, interface, tensile, and bending strengths by increasing the length of the geocell layer.

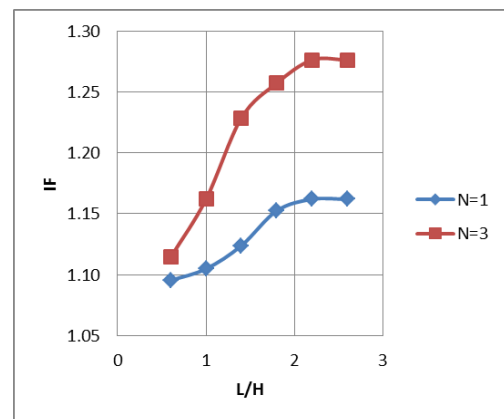


Figure 10. Variations of slope improvement factor affected by the length of the reinforcement layer

As indicated in Fig. 11, the displacement of the slope is reduced by lengthening the geocell layer. Increasing L/H ratio from 0.6 to 2.6 in a geocell layer, the displacement is reduced by 7.32%. Furthermore, the displacement is declined by 13.81% in three geocell layers. At L/H=1.8, as the

number of layers increases from 1 to 3, the displacement is reduced by 15.2%.

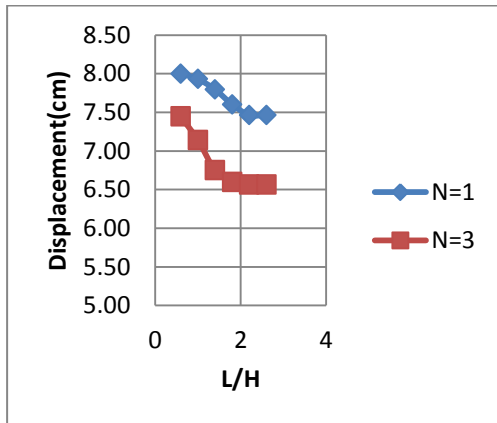


Figure 11. Variation of slope displacement affected by the length of the reinforcement layer

Increasing L/H from 0.6 to 2.6 in one geocell layer, the axial force is reduced in geocell by 7%. Moreover, it is reduced by 14.44% in the other three layers of geocell. At L/H=2.6, increasing the number of layers from 1 to 3, the axial force is declined by 5.18%. The effect of length on three layers of geocell is more tangible than on one layer of geocell (Fig. 12).

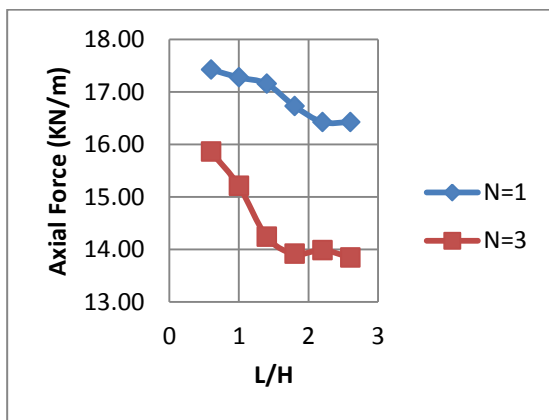


Figure 12. Variation of axial force of geocell layer affected by the length of the reinforcement layer

According to the investigation of the bending moment, it is declined approximately by 7% and 11.4% in one and three geocell layers, respectively. At L/H=2.6, the bending moment is reduced by 20% by increasing the number of geocell layers (Fig. 13).

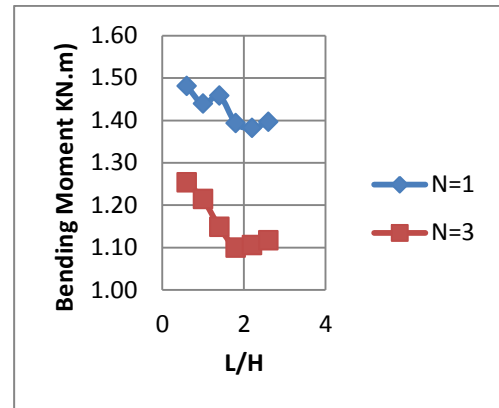


Figure 13. Variation of the bending moment in the geocell layer affected by the length of the reinforcement layer

6. Effect of Suction Variations on the Stability of the Reinforced Slope

The stability of reinforced slope is investigated for one geocell layer at the suctions of 20kPa and 55Kpa (Since the water-soil curve has changed).The effect of suction variations is more tangible on the slope stability. As it can be observed in Fig.14, increasing the suction, the slope improvement factor is escalated by 21.2%. Moreover, at u/H=0.6, the slope improvement factor experiences a descending trend of about 10% at a constant suction that finally takes the values of a non-reinforced slope at u/H=1 (Fig. 14).

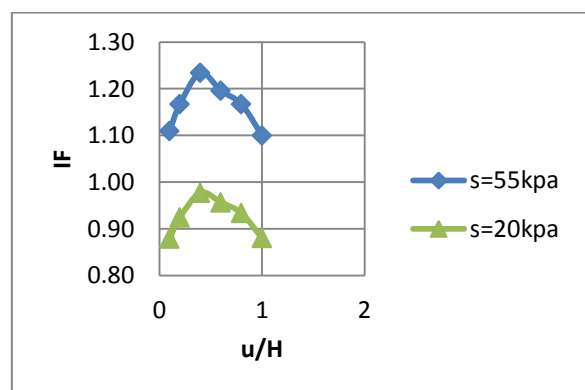


Figure 14. Changes of slope improvement factor affected by suction variations

As seen in Fig. 15, the maximum displacement has occurred at u/H=1 in the geocell sublayer where the geocell layer produces no effect on restraining the forces induced by soil weight. On the other

hand, if the geocell layer has a substantial depth from the slope surface ($u/H=1$), the lateral vertical displacement of slope increases at the upper part of the slope and all displacement occurs at the upper part of the slope. This results in the reduction of a factor of safety of slope where the slope has a behavior identical to a non-reinforced slope. At $u/H=0.2$, the suction increase has yielded a reduction in the displacement by 17.9% which is the least increase among other ratios of u/H .

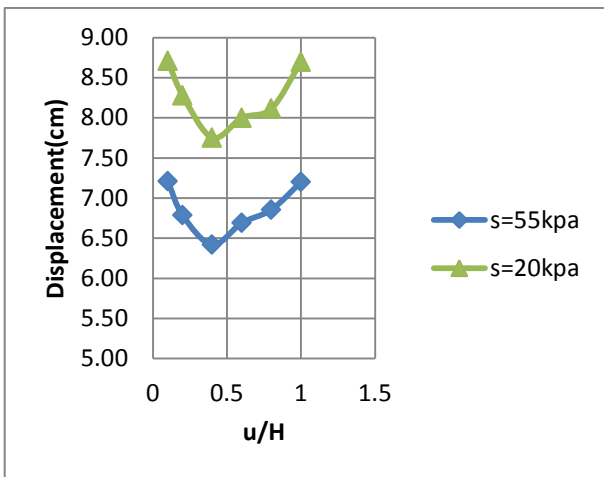


Figure 15. Variations of slope displacement affected by the suction change

The first geocell layer significantly transfers forces to the lower parts and consequently leads to the force transfer to other geocell layers, enhancing the stability performance. Also, the obtained results show that as the overhead pressure increases, the axial force increases in the geocell reinforcement while the bending moment goes down. Increasing suction, geocell axial force declines by at most 18.5%. As overhead pressure increases, there is an increase in the force concentrated at the soil-geocell interface and the tensile force is consequently enlarged in reinforcements. Therefore, as the first geocell layer receives most of the forces, the bending moment is mainly concentrated in the first geocell layer and it consequently decreases in other layers. The suction increase immensely affects slope stability (Fig. 16).

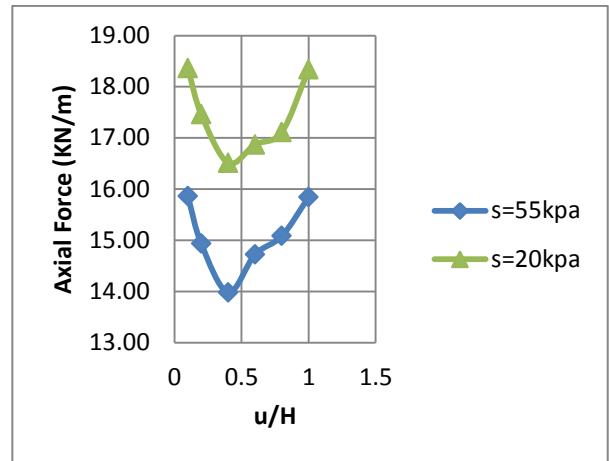


Figure 16. Variation of the axial force of the geocell layer affected by the suction change

By increasing the height of the geocell layer, the moment of inertial increase and, consequently; the bending moment of geocell reinforcement increases as well. In this condition, the behavior of the geocell layer is identical to a deep beam, reducing the reinforcement deformation and consequently declining the lateral deformation of the slope. On the other hand, the reinforcement efficiency is dramatically dropped by decreasing the height of the geocell layer.

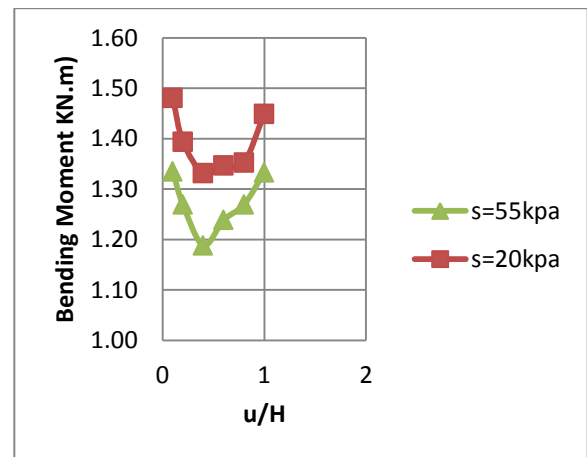


Figure 17. Variations of the bending moment in the geocell layer affected by the suction change

Until $u/H=0.4$, the bending moment experiences a descending trend. Nevertheless, in this state, the bending moment has an ascending trend of up to 11.7% by increasing suction (Fig. 17).

7. Comparison of FOS in the Barcelona Basic Model and Cam Clay Model.

Fig.18 shows the variations of FOS of slope affected by the Barcelona Basic Model and Cam Clay Model in saturated soil conditions. As seen, the results based on the Barcelona basic model are more conservative than the cam clay model. In saturation soil conditions, the coefficient FOS to 60% decreases relative to unsaturated soil conditions. The reason for this is to consider the suction in unsaturated conditions. At $u/H=1$, reinforced Slopes and unreinforced slope are equal. In fact, the saturation conditions are the most critical condition of the slope.

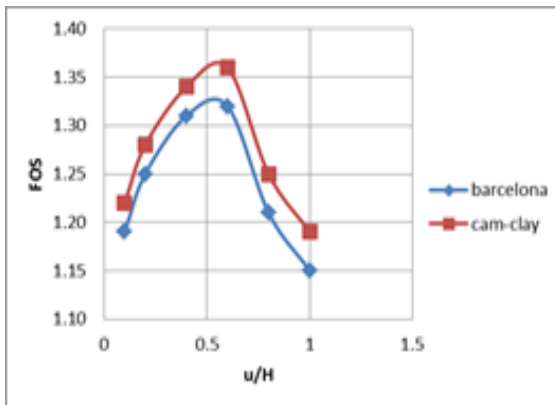


Figure 18. Variations in the FOS of slope against the Soil behavior model.

8. Conclusion

The obtained results reveal that the effective embedment depth of the geocell layer is at the middle of slope height and the increase in the number of geocell layers has a larger effect on the slope stability compared to the increase in the geocell length. By placing the first geocell layer in the effective zone, the development of failure surfaces is reduced and they are transferred to a deeper depth. To that end, other geocell reinforcements also behave like a slab receiving vertical pressures from the top layer and transferring them to deeper depths of soil. In fact, the first layer causes the relationship between the geocell layers so as to transport the stress. If the length of the geocell layer is small compared to the sliding surface, the resistant bending moment of

the geocell layer will be negative. This is due to the very small magnitude of resistant moment formed by the tensile force of the geocell layer. The negative bending moment of the geocell layer yields an increase in the lateral displacement of slope and also the displacement of the geocell layer.

The effective length of the reinforcement layer equals the length of the geocell layer located inside the sliding surface where there is a large extent of tensile, shear, and bending forces of the geocell layer. On the other hand, the length of the reinforcement layer must be a little larger than the sliding surface length to avoid the probable propagation of sliding surfaces and also to provide an appropriate restraining length to deal with the reinforcement layer pullout against the applied forces. The enhancement rate of the factor of safety with respect to the number of geocell layers largely depends on the depth of the first reinforcement layer. This is attributed to the ability of the first reinforcement layer to avoid the propagation of sliding surface which can consequently affect the overall slope stability. The performance of other geocell layers can be largely associated with the enhancement of the later deformation of the slope. Furthermore, by increasing the length of geocell reinforcement, the generated moment of inertia is declined and, as a result, the bending moment of reinforcement is also reduced. This way, the behavior of geocell reinforcement approaches the behavior of plate reinforcement, leading to a decrease in efficiency.

As the suction increases, the factor of safety of slope increases leading to the lower displacement and stability of the reinforced slope. The presence of matric suction in the structure of unsaturated soil brings about a higher strength and stability of the soil. Furthermore, by declining the saturation degree, the matric suction increases in the soil structure leading to a more enhanced factor of safety. Indeed, in comparison to the increase in the length and number of geocell layers, the suction increase has a sharper effect on the slope stability.

References

- [1] Sheng, D., "Review of fundamental principles in modelling unsaturated soil behavior"; Computers and Geotechnics; 38, pp.757-776, 2011.
- [2] Sheng, D., "Constitutive Modelling of Unsaturated Soils: Discussion of Fundamental Principles."; Unsaturated soils; 1, 91-112, 2011.
- [3] Sangseom, J.Yongmin, K, "Effects of rainfall infiltration and hysteresis on the settlement of shallow foundations in unsaturated soil"; Environmental Earth Sciences, 77:494, 2018.
- [4] Fredlund, D.G., Morgenstern N.R., Widger A., "Shear strength of unsaturated soils"; Can. Geotech. J; 15, pp.313-321, 1978.
- [5] Wu LZ, Huang RQ, Xu Q, Zhang LM, Li HL., "Analysis of physical testing of rainfall-induced soil slope failures". Environ Earth Sci 73:8519-8531, 2015.
- [6] Oberg, A. L., Salfors, G.A., "rational approach to the determination of the shear strength parameters of unsaturated soils"; Proc. 1st Intl Conf. Unsaturated Soils, Paris, pp.151-158, 2, pp. 279-289, 1996.
- [7] Kim Y, Jeong S, Kim J .Coupled infiltration model of unsaturated porous media for steady rainfall. Soils Found 56(6):1073-1083, 2016.
- [8] Ma T, Li C, Lu Z, Bao Q., "Rainfall intensity-duration thresholds for the initiation of landslides in Zhejiang Province", China. Geomorphology 245:193-206, 2015.
- [9] Khalili, N., Khabbaz, M. H., "A unique relationship for χ for the determination of the shear strength of unsaturated soils"; Geotechnique; 48, No .5, pp.681-687, 1998.
- [10] Alonso, E.E., Gens, A., josa, A., "A constitutive model for partially saturated soils" Geotechnique; 40, pp.405-430, 1990.
- [11] M.Isabel, M.Pinto, T.W.Cousens., "Geotextile Reinforced Brick Faced Retaining Walls", Geotextiles and Geomembranes, 14 - 449-464, 1996.
- [12] Wu LZ, Selvadurai APS. Rainfall infiltration-induced groundwater table rise in an unsaturated porous medium. Environ EarthSci 75(2):1-11, 2016.
- [13] Graeme, D. Skinner, R. Kerry Roweb, "Design and behaviour of a geosynthetic reinforced retaining wall and bridge abutment on a yielding foundation", Geotextiles and Geomembranes, 23(3), pp.234-260, 2005.
- [14] Jorg G. Zornberg, Nicholas Sitar, James K. Mitchell, Honorary Member., "Performance of Geosynthetic Reinforced Slopes at Failure", Journal of Geotechnical and Geoenvironmental Engineering, 1998.
- [15] Jorge, G. Zornberg, M.ASCE, Fabiana Arriag., "Strain Distribution within Geosynthetic-Reinforced Slopes", Journal of Geotechnical and Geoenvironmental Engineering, 129(1),32-45, 2003.
- [16] Lazhar, B., Hacene B., Jarir Y. "Internal Stability Analysis of Reinforced Earth Retaining Walls", Geotech Geol Eng, 29:443-452,2011.
- [17] Chen, R.H., Chiu, Y.M. "Model Tests of Geocell Retaining Structures", Geotextiles and Geomembranes 26 (1),pp.56-70, 2008.
- [18] Chen, R.H., Huang, Y.W., Huang, F, C., "Confinement Effect of Geocells on Sand Samples Under Triaxial Compression", Geotextiles and Geomembranes, 37(1), pp. 35-44, 2013.
- [19] Fakher A. and Jones C.J.F.P., "When the bending stiffness of geosynthetic reinforcement is important". Geosynthetics International, 8, No. 5, 445-460,2001.
- [20] Zhang L, Zhao MH, Zou XW, Zhao H., "Deformation analysis of geocell reinforcement using winkler model". Comput Geotech;36:977-83, 2009.
- [21] Zhang, L., Zhao, M.H., Zou X.W. and Zhao, H., "Analysis of geocell reinforced mattress with consideration of horizontal vertical coupling". Comput Geotech, 37, 748-56,2010.
- [22] Dash, S.K., Rajagopal, K., Krishnaswamy, N.R., "Behaviour of geocell reinforced sand beds under strip loading". Canadian Geotechnical Journal 44, 905-916, 2007.
- [23] Yang, X. M., Han, J., Parsons, R. L., and Leshchinsky, D., "Threedimensional numerical modeling of single geocell-reinforced sand." Front.Archit. Civ. Eng. China, 4(2), 233-240, 2010.
- [24] Van Genuchten MY., "A closed form equation for predicting the hydraulic conductivity of unsaturated soils". Soil Sci Soc Am J 44:892-898, 1980.
- [25] Sreedeeep S, Singh DN., "Nonlinear curve-fitting procedures for developing Soil-water characteristic curves". Geotech Test J 29(5):409-418, 2006.
- [26] Y.M. Cheng a, T. Lansivaara b, W.B. Wei."Two-dimensional slope stability analysis by limit

equilibrium and strength reduction method".
Computers and Geotechnics 34, 137–150, 2007.

- [27]Madhavi Latha, G., Rajagopal, K. and Krishnaswamy, N.R. "Experimental and theoretical investigations on geocell supported embankments" International Journal of Geomechanics. ASCE, Vol.6, pp.30-35, 2006.
- [28]Mehdipour, I., Ghazavi, M., Moayed, R.Z. "Numerical study on stability analysis of geocell reinforced slopes by considering the bending effect". Geotext. Geomembr. 37, 23e34, 2013.